Hurpin Is a Selective Inhibitor of Lysosomal Cathepsin L and Protects Keratinocytes from Ultraviolet-Induced Apoptosis†

Thomas Welss,‡ Jiuru Sun,§ James A. Irving,§,|| Rainer Blum,‡ A. Ian Smith,⊥ James C. Whisstock,§,|| Robert N. Pike,§ Anna von Mikecz,# Thomas Ruzicka,‡ Phillip I. Bird,§,▽ and Harry F. Abts*,‡,▽

Department of Dermatology, Heinrich Heine University, D-40225 Düsseldorf, Germany, Department of Biochemistry and Molecular Biology and Victorian Bioinformatics Consortium, Monash University, 3800 Monash, Australia, Baker Medical Research Institute, St Kilda Central 8008, Australia, and Institut für umweltmedizinische Forschung, Heinrich Heine University, D-40028 Düsseldorf, Germany

Received December 5, 2002; Revised Manuscript Received March 26, 2003

ABSTRACT: Hurpin (headpin/PI13/serpinB13) is an intracellular, differentially spliced member of the serpin superfamily that has been linked to differentiation and apoptosis of human keratinocytes. It is transiently downregulated by UV light and overexpressed in psoriatic skin lesions. Although it has all of the features of an inhibitory serpin, a productive interaction between hurpin and a proteinase has not yet been reported. Here we demonstrate that hurpin is a potent and selective inhibitor of the archetypal lysosomal cysteine proteinase cathepsin L (catL). Recombinant hurpin inhibits human catL with a stoichiometry of inhibition (SI) of 1.7 and a rate constant k_{assoc} of $(4.6 \pm 0.14) \times 10^5$ M^{-1} s^{-1}. It inefficiently inhibits catV and does not inhibit papain, catB, or catK. To investigate the inhibitory mechanism, we determined the P1−P1′ bond in the reactive center loop cleaved by catL (^{356}Thr−^{357}Ser) and expressed variants in which the proximal hinge, P1 residue, or differentially spliced CD loop was mutated. The results of assays using these proteins suggest that inhibition of catL by hurpin occurs via the conventional serpin inhibitory mechanism and that the CD loop plays no role in the process. Finally, it was found that the majority of hurpin is cytosolic and that its overexpression in human keratinocytes confers resistance to UV-induced apoptosis. Given that lysosomal disruption, release of catL, and catL-mediated caspase activation are known to occur in response to cellular stress, we propose that a physiological role of hurpin is to protect epithelial cells from ectopic catL.

Proteinase inhibitors belonging to the serpin superfamily are characterized by distinct structural and mechanistic properties (*1*, *2*). Serpins contain three β-sheets and nine α-helices in a characteristic three-dimensional conformation. The exposed reactive center loop (RCL)[1] functions as a bait or pseudosubstrate for the target proteinase. Cleavage of the RCL between the P1 and P1′ residues causes a conformational change in the serpin, the so-called stressed to relaxed transition, in which residues N-terminal to the cleaved bond insert into β-sheet A. This conformational change translocates the proteinase to the opposite pole of the serpin, distorts its catalytic site, and results in a covalently linked, stable complex between inhibitor and proteinase (*3*).

Hurpin (HaCaT UV-repressed serpin; PI13; serpinB13) is a member of the ovalbumin (ov) or intracellular branch of the human serpin family and was originally discovered as a UV-repressible gene by differential display analysis of the UV-modulated gene expression in human keratinocytes (*4*, *5*). It was independently described on the basis of its differential expression in head and neck cancer and named headpin (*6*).

Hurpin shares all of the features of ov-serpins (*7*), including localization to one of the two ov-serpin gene clusters, and a genomic organization typical of a chromosome 18q21.3 serpin (*8*, *9*). In particular, it possesses the characteristic "CD loop" between helix C and helix D (*7*, *10*). This loop can interact with other proteins independently of the RCL (*11*). For example, bomapin carries a nuclear targeting signal in this region (*12*). In hurpin it appears that differential splicing generates variants with CD loops of different lengths (*8*); however, the functional significance of these variants is unknown.

The physiological role of hurpin has yet to be elucidated, and in particular a cognate target proteinase has not yet been identified. The inhibitory specificity of a serpin that inhibits

† This work was supported by the Deutsche Forschungsgemeinschaft (DFG) within the Sonderforschungsbereich 503 Project A1 (grants to T.R. and H.F.A.), by the Australian Research Council, and by the National Health and Medical Research Council of Australia (grants to P.I.B., R.N.P., and J.C.W.).

* Address correspondence to this author at Cardion AG, Max-Planck-Str. 15a, D-40699 Erkrath, Germany. Fax: +49-211-205-65-98. Tel: +49-211-205-65-84. E-mail: abts@cardion.de.

‡ Department of Dermatology, Heinrich Heine University.

§ Department of Biochemistry and Molecular Biology, Monash University.

|| Victorian Bioinformatics Consortium, Monash University.

⊥ Baker Medical Research Institute.

Institut für umweltmedizinische Forschung, Heinrich Heine University.

▽ These authors contributed equally to the work.

[1] Abbreviations: catB, cathepsin B; catK, cathepsin K; catL, cathepsin L; catV, cathepsin V; crmA, cytokine response modifier A; eGFP, enhanced green fluorescent protein; hurpin, HaCaT UV-repressed serpin; MENT, myeloid and erythroid nuclear termination stage-specific protein; RCL, reactive center loop; serpin, serine proteinase inhibitor; SCCA, squamous cell carcinoma antigen; TUG, transverse urea gradient; UV, ultraviolet light.

10.1021/bi027307q CCC: $25.00
Published on Web 06/03/2003

serine proteinases is mainly dictated by the P1−P1′ residues in the RCL, and from sequence alignments these residues in hurpin are Thr^{356}−Ser^{357}, respectively (*5*, *6*). The hinge region of hurpin exhibits high identity to the postulated consensus sequence EEGTEAAAAT (P17−P8) for inhibitory serpins (*13*, *14*), suggesting that it has the capacity to inhibit proteinase activity.

Previous analysis of the interaction of hurpin with common serine proteinases using in vitro translated protein failed to demonstrate an SDS-stable complex (*5*) typical of serpin−proteinase interaction (*15*). However, interaction of hurpin with the cysteine proteinases cathepsin B (catB) and cathepsin L (catL) showed limited cleavage of the serpin, possibly in the RCL, without the appearance of an SDS-stable complex (*5*). Since SDS-stable complexes do not necessarily result from serpin-mediated cysteine proteinase inhibition (*16*, *17*), we were interested to see if hurpin possesses inhibitory activity against cysteine proteinases. Here we show that hurpin is a potent and selective inhibitor of lysosomal cathepsin L; in fact, it is the most specific serpin interaction with a cysteine protease characterized to date. It is likely that this specificity is primarily due to the presence of valine at the P_2 position, leading to a fine balance between optimal inhibitory activity and narrow target specificity.

MATERIALS AND METHODS

Cloning the Hurpin Coding Sequence in a Yeast Expression Vector. The complete hurpin coding sequence was amplified from the λ cDNA clone 1.1 (EMBL accession no. AJ001696) using a high-fidelity Taq system (Roche, Mannheim, Germany) and primers designed to incorporate *Eco*RI sites. Via the 5′-PCR primer the hurpin cDNA was modified to encode six histidine residues at the N-terminus. The gel-purified 1159 bp fragment was *Eco*RI digested and cloned into the *Eco*RI site of pHIL-D2 (Invitrogen). Correct orientation and sequence were confirmed by sequencing of the recombinant plasmid.

Generation of Hurpin Mutants. Hurpin cDNA in the expression vector pHIL-D2 was mutated by the method of Deng and Nickoloff (*18*). Primers were designed to mutate the hurpin sequence in the proximal hinge region from ^{343}Thr to ^{343}Arg (hinge mutant) and the putative P1−P1′ site from ^{356}Thr to ^{356}Ala (P1 mutant) and to delete the CD interhelical loop (CD mutant). These alterations and the absence of second-site mutations were confirmed by DNA sequencing. The recombinant mutant hurpin proteins were expressed in the methylotropic yeast *Pichia pastoris* as described below.

Purification of Recombinant Yeast Hurpin. The hexahistidine-tagged hurpin was produced in the methylotropic yeast *P. pastoris* using procedures described previously (*19*). Briefly, expression of recombinant protein was controlled by the *P. pastoris* alcohol oxidase promoter and induced with methanol. Following cell lysis recombinant hurpin was separated from yeast proteins by affinity chromatography using the metal affinity resin Talon (Clontech, Palo Alto, CA). Further purification of hurpin was performed by ion-exchange chromatography using HiTrap DEAE-Sepharose columns (Pharmacia, Freiburg, Germany) equilibrated in 20 mM Tris at pH 7.5. Columns were eluted with a gradient of 0−100% high-salt buffer (20 mM Tris, 500 mM NaCl, pH 7.5) over 40 min at 1 mL/min. Protein purity was assessed by SDS−PAGE visualized by Coomassie blue staining (Bio-Rad, Munich, Germany). Concentrations of proteins were determined by absorbance at 280 nm or using the Nano Orange protein quantification kit (Molecular Probes).

Analysis of Thermodynamic Properties by Transverse Urea Gradient (TUG) Gel Electrophoresis Analysis. Hurpin (100 μg) was size-separated in a TUG gel with a 0−8 M urea gradient as described (*20*). After electrophoresis, the proteins were visualized by staining with Coomasie blue R-250 (Bio-Rad, Munich, Germany).

Identification of the P_1−P_1' Bond. Peptides resulting from the cleavage of recombinant hurpin by catL were purified and sequenced as described previously (*21*).

Assays for Inhibition: Proteinases, Substrates, and Assay Buffer. Papain, human cathepsin L (catL), and human cathepsin B (catB) were purchased from Calbiochem (Darmstadt, Germany), and the substrates *N*-Cbz-Phe-Arg-AMC (Cbz-FR-AMC) and Z-Arg-Arg-AFC were purchased from Sigma (St. Louis, MO). Human cathepsin V (catV) and cathepsin K (catK) were obtained from Dr. D. Brömme (Mount Sinai School of Medicine, New York) or prepared using expression systems constructed previously (*22*, *23*). Active enzyme concentration was determined by titration with the inhibitor E-64 (*24*). Kinetic assays were conducted in cathepsin buffer (0.1 M acetate, pH 5.5, 1 mM EDTA, 0.1% Brij35, 10 mM cysteine) using the fluorescent substrate Cbz-Phe-Arg-AMC. Prior to being assayed, enzymes were preactivated for 15 min in cathepsin buffer. Assays were performed on a BMG Fluorostar plate reader (BMG, Germany) or on a Fluoroskan Ascent (ThermoLifeSciences, Egelsbach, Germany).

Trypsin, thrombin, and chymotrypsin were purchased from Sigma (St. Louis, MO). Neutrophil elastase was from Athens Research Technology (Athens, GA). Recombinant human granzyme B and the granzyme B substrate Abz-IEPDSS-MESK-Dnp were as described (*21*). The substrates Boc-VPR-AMC and *N*-succinyl-AAPF-AMC were purchased from Sigma (St. Louis, MO). Analyses of the interaction of hurpin and serine proteinases were carried out using methods described in ref *21* and references cited therein.

Stoichiometry of Inhibition (SI). The SI of the interaction between hurpin variants and cysteine proteases was determined as described previously (*25*). Briefly, 10 nM protease was incubated with different concentrations of inhibitor (at up to a 40-fold excess) at 37 °C for 30−45 min in cathepsin buffer, and fractional residual activity was plotted against the inhibitor:enzyme ratio. Extrapolation to the intercept corresponding with complete loss of activity yielded the SI value.

Second-Order Association Rate Constant (k_{assoc}). The second-order association rate constant (k_{assoc}) was determined under pseudo-first-order conditions, as described (*26*, *27*). Briefly, a constant amount of enzyme was incubated with a 10−75-fold excess of inhibitor in cathepsin buffer. Reactions (final volume, 200 μM) were followed continuously for 2 h at 30 °C using 20 mM Cbz-FR-AMC substrate. The first-order rate constants (k_{obs}) were calculated by a nonlinear regression fit to an equation describing slow, tight binding (*28*):

$$P = V_s t + (V_z - V_s)(1 - e^{-k_{obs}t})/k_{obs}$$

where product formation (P) proceeds at an initial velocity (V_z) and is inhibited over time (t) at rate k_{obs} until the reaction reaches a new steady-state velocity (V_s). The slope of the linear regression through a plot of k_{obs} against inhibitor concentration yielded the uncorrected second-order association rate constant (k_{unc}). Finally, this was adjusted for the K_m of the interaction of protease with substrate (S):

$$k_{assoc} = k_{unc}(1 + [S]/K_m)$$

Transient Expression of an eGFP-Hurpin Fusion Protein in HaCaT Cells. The hurpin coding sequence was obtained from a hurpin cDNA template by PCR amplification using a proofreading Taq polymerase [expand high-fidelity PCR enzyme mix (Roche, Mannheim, Germany)]. The PCR-generated hurpin CDS was cloned into pEGFP-C1 and pEGFP-N1 utilizing the *Xho*I (5′) and *Sma*I (3′) restriction sites of the vectors. The restriction sites flanking the hurpin CDS were introduced during PCR by appropriately designed primers.

Plasmid DNA for transfection was isolated using the EndoFree plasmid maxi kit (Quiagen, Hilden, Germany). Transfection of the plasmid DNA into the human keratinocyte cell line HaCaT (*29*) was performed by nucleofection using a Nucleofector device (setting U20) and cell line Nucleofector kit V (Amaxa, Cologne, Germany) according to manufacturer's instructions. HaCaT cells were cultivated after transfection in a humidified atmosphere at 37 °C with 5% CO_2 using DMEM supplemented with 10% endotoxin-reduced FCS. Cells were analyzed in 10 cm culture dishes using a fluorescence microscope (Axioplan; Zeiss, Göttingen, Germany) equipped with a water immersion objective (Zeiss Achroplan, 40×/0.8 W) and FITC filter set.

Confocal Laser Scanning Microscopy (CLSM). HaCaT cells transfected with pEGFP-N1-hurpin were plated on gelatin (0.1%) coated soda lime glass Lab-Tek chamber slides (Nalge Nunc, Naperville, IL) and cultured for 24 h. Cells were mounted in DAKO fluorescent mounting medium (DAKO, Hamburg, Germany) to reduce fading of the fluorescent signal.

Optical sections of cells expressing eGFP-hurpin were generated using a confocal laser scanning microscope from Olympus (Fluoview 2.0, IX70 inverted microscope). A 488 nm laser line of an argon laser was used to excite eGFP. Confocal stacks of single cells were recorded with a pinhole setting of 2. Digitalized image information was visualized using Adobe Photoshop.

Analysis of UV-Induced Apoptosis in Stable Transfected HaCaT Cells. The PCR-generated and gel-purified hurpin CDS was inserted via TA cloning into pcDNA3.1/V5/His-TOPO (Invitrogen, Karlsruhe, Germany). HaCaT cells were transfected with EndoFree (Quiagen) purified plasmid DNA on 10 cm culture dishes using Lipofectamine Plus according to the manufaturer's protocol. Three days after transfection selection of plasmid-containing cells was started by adding G418 (0.5 mg/mL) to the culture media. After 14 days of antibiotic selection, single resistant clones of cells with stable integrated plasmids were obtained. Individual clones were transferred initally to 24-well plates and expanded for the UV irradiation on 10 cm dishes.

UV irradiation was performed as previously described (*30*). For measuring apoptosis caspase 3 (CPP32) activity was monitored using the ApoAlert CPP32 assay kit (Clontech). Cleavage of the substrate (DEVD-AFC) by caspase 3 was measured fluorometrically using the Fluoroskan Ascent microplate reader (ThermoLifeSciences, Egelsbach, Germany) with 390 and 538 nm for excitation and emission, respectively.

Modeling. A homology model of hurpin, based on the crystal structure of ovalbumin [PDB accession no. 1OVA (*31*)], was constructed using the MODELLER program (*21*, *32*) and the QUANTA package (MSI Inc.).

RESULTS

Expression and Purification of Recombinant Hurpin. For large-scale production of recombinant protein, hurpin was expressed in the methylotropic yeast *P. pastoris*. To simplify purification, the recombinant protein was produced as an N-terminal hexahistidine-tagged protein, which was separated from yeast proteins by cobalt affinity chromatography. This step resulted in marked enrichment of hurpin (Figure 1A), which was further purified by ion-exchange chromatography using a high-salt buffer for elution (Figure 1B). Typically, hurpin eluted at 120−150 mM NaCl as a single absorbance peak at 280 nm.

Because hurpin has no known proteinase partner that could be used to assess the functional integrity of the recombinant protein, we used transverse urea gradient (TUG) gel analysis (*20*) to check that the purified material exhibits the unfolding characteristics of functional inhibitory serpins. This assesses the unfolding transition between the folded and unfolded states. Inhibitory serpins show a rapid transition between the folded (native/stressed *S*-form) and the unfolded (denatured/relaxed *R*-form) form, which results in a sigmoidal band in the TUG gel. As shown in Figure 1C, the recombinant hurpin demonstrated a sigmoidal migration pattern in this system. We concluded that the yeast-generated hurpin is active and able to undergo the stressed to relaxed transition essential for inhibitory function.

Inhibitory Capacity of Hurpin. By sequence analysis hurpin is predicted to possess the conserved features of inhibitory serpins, such as the hinge regions flanking the RCL which promote the flexibility of this crucial part of the inhibitor. It also possesses a CD loop, which in some serpins modulates conformational change and inhibitory activity or dictates cellular localization. A model of hurpin based on the structure of ovalbumin (Figure 2A) illustrates the relative positions of the RCL and the CD loop. Figure 2B illustrates several important features present in the RCL of hurpin: (1) a sequence motif in the hinge region that is characteristic of an inhibitory serpin (*33*); (2) a bulky, hydrophobic valine residue in the P_2 position (the primary determinant of cysteine proteinase specificity); and (3) a proline in the P_3' position, which is predicted in SCCA-1 to interact with a tryptophan residue within the active site cleft of cysteine proteinases (*34*).

Previous studies using in vitro translated hurpin against a panel of serine proteinases failed to demonstrate SDS-stable complex formation (*5*). These investigations were repeated using recombinant hurpin, but no inhibition could be demonstrated, either by complex formation or by kinetic analysis (Table 1). By contrast, the original experiments showed that incubation with several cathepsins leads to

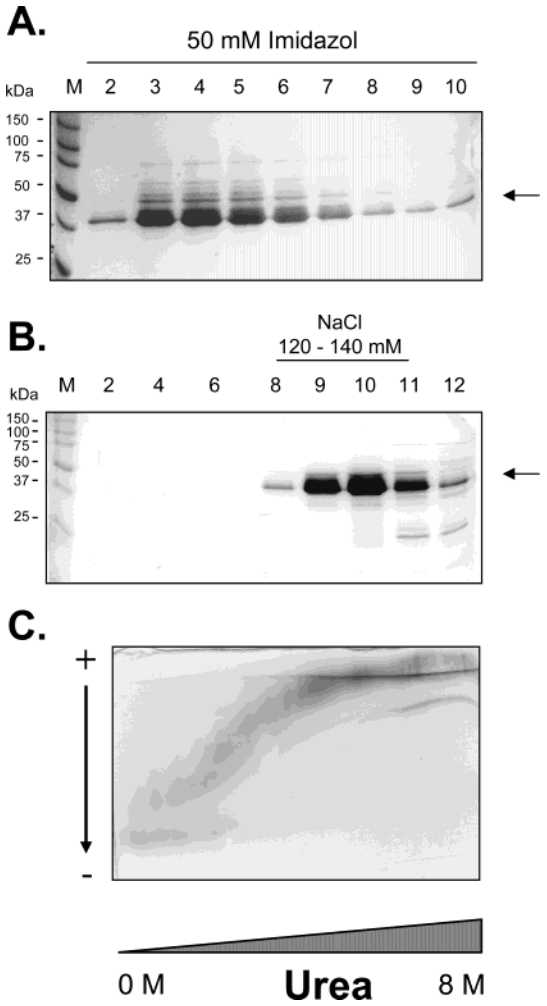

FIGURE 1: Purification of recombinant hurpin from yeast. (A) Hurpin containing an N-terminal His tag was partially purified from yeast lysate by metal chelate affinity chromatography. Aliquots of the indicated fractions eluted with 50 mM imidazole have been size separated in a 12.5% PAA gel. (B) Further purification was achieved by anion-exchange chromatography. Numbers indicate consecutive collected fractions. Separation was performed in a 12.4% PAA gel. Proteins in (A) and (B) have been visualized by Coomassie blue staining. The arrow indicates the position of the yrhurpin. M denotes the lane with size markers. Molecular masses of the marker bands are given on the left in kilodaltons. (C) To test the functional integrity of the recombinant hurpin, the purified protein was separated in a gel containing a urea gradient (0−8 M) perpendicular to the electric field.

shortening of in vitro translated hurpin by approximately 4 kDa, which is consistent with cleavage in the RCL (*5*). Given that serpin−cysteine proteinase complexes are not usually SDS-stable and that sequence analysis predicted that hurpin is a cysteine proteinase inhibitor (Figure 2B), we performed an initial screen of inhibitory activity against cathepsins B, L, K, and V and papain using up to a 40-fold excess of hurpin (Table 1). Hurpin demonstrated no significant inhibitory activity against papain, cathepsin B, or cathepsin K. In contrast, partial inhibition of cathepsin V was observed at an inhibitor:enzyme ratio of 8, and a 5-fold molar excess of hurpin inhibited cathepsin L completely. To confirm specific inhibition of catL and catV by hurpin and distinguish the observed inhibition from a simple substrate reaction, more detailed kinetic studies were performed. A characteristic feature of serpin inhibition is the formation of a tight complex with the proteinase at a unimolar stoichiometry. Alternatively, if the proteinase cleaves the serpin too rapidly or outside the normal P1−P1′ bond, the interaction follows the substrate pathway, resulting in inactivation of the serpin and failure to form the complex. The stoichiometry of inhibition (SI) indicates the extent to which the inhibitor−enzyme complex follows the substrate rather than the inhibitory pathway. Use of this parameter with hurpin is justified in light of evidence that complex formation for serpin-mediated inhibition of cysteine proteinases is identical to that for serine proteinases (*25*, *35*) and the observation that hurpin's inhibitory behavior is consistent with this (see below). The SI of the interaction between hurpin and cathepsin L was found to be 1.7, whereas that for cathepsin V was 17. These results indicate that most of the hurpin−cathepsin L complex follows the inhibitory pathway, whereas most of the hurpin−cathepsin V complex follows the substrate pathway. Thus hurpin is a reasonably efficient inhibitor of the former but not the latter. These initial data indicate that cathepsin L may be a target proteinase for hurpin; we therefore asked if the rate of complex formation is in the physiological range ($>10^4$ M^{-1} s^{-1}) (*36*). The second-order association rate constant was found to be (4.6 ± 0.14) $\times$ 10^5 M^{-1} s^{-1}, comparable to reported rates for physiologically relevant serpin−serine proteinase interactions.

Determination of the catL Cleavage Site in the Hurpin RCL. Specific cleavage of the RCL between two residues designated P1 and P1′ is an essential part of the inhibitory mechanism and occurs early in the serpin−proteinase interaction. Sequence comparisons suggest that the consensus P1 residue in hurpin is ^{356}Thr. To confirm this, recombinant hurpin was incubated with catL, and the cleavage products around the predicted size (4−6 kDa) were purified by HPLC and sequenced. As shown in Figure 3, sequences were obtained for four peptides. Of these, one yielded a sequence from ^{357}Ser (SAPGHENV), indicating that catL cleaves hurpin at the predicted P1 position in the RCL. The other sequences comprised an unknown (neither hurpin nor catL), the N-terminal His tag of hurpin, and a sequence beginning at ^{70}Ala in hurpin (AEEKEVIE). This last sequence is part of the interhelical CD loop. The appearance of other products due to cleavage outside the RCL suggests that catL-sensitive regions are exposed when hurpin undergoes the stressed to relaxed transition during inhibition or that those hurpin molecules that follow the substrate pathway are cleaved at multiple positions by catL.

Inhibitory Mechanism of Hurpin. To date there are only a limited number of studies addressing the similarities and differences between serine proteinase and cathepsin inhibition by serpins (*34*, *35*), implicating that in both types of inhibition the serpin−RCL plays an important role. To investigate the mechanisms underlying inhibition of catL by hurpin, we therefore generated several hurpin variants in which crucial functional elements were changed, especially those in the RCL (summarized in Table 2).

(A) P1 Mutant. The specificity of papain-like cysteine proteinases is primarily determined by the P2 position, whereas that for the interaction between a serpin and its cognate serine proteinase is primarily determined by the P1 residue. To investigate how perturbable the interaction between hurpin and cathepsin L is, we mutated ^{356}Thr (identified in this report as the P1 residue) to ^{356}Ala. The resulting P1 mutant inhibitor was active but, surprisingly,

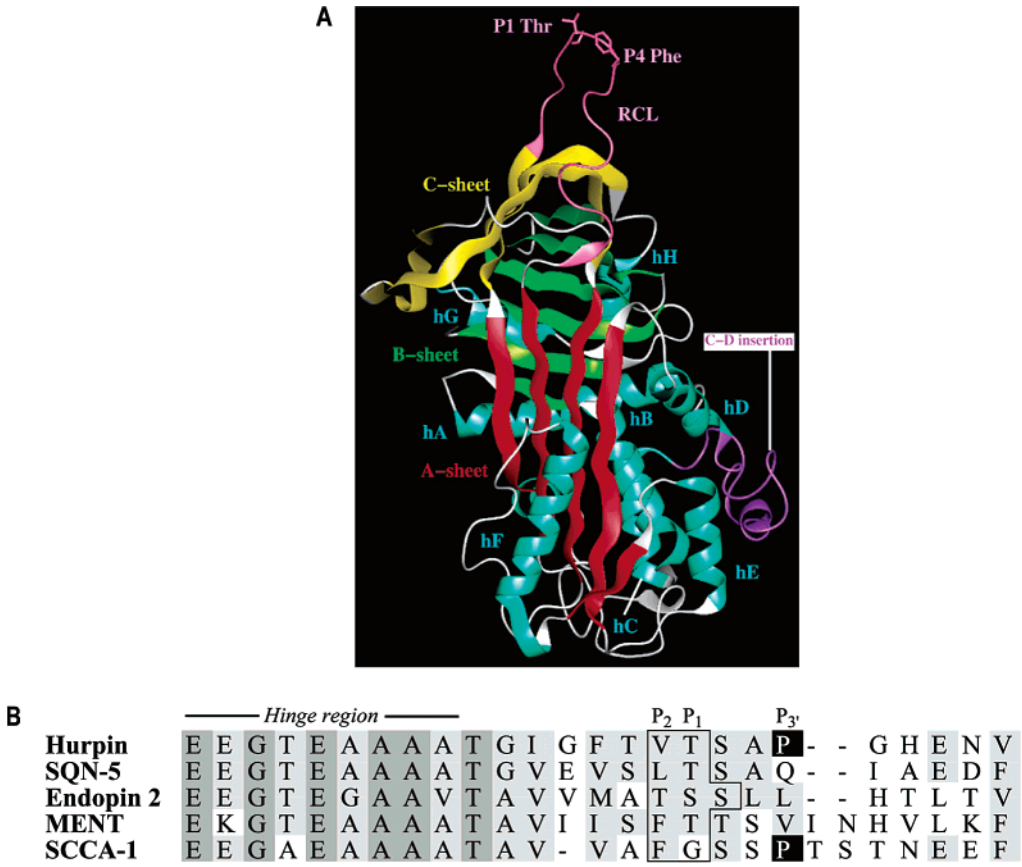

FIGURE 2: Model of hurpin and sequence alignment of the hurpin RCL with other serpins. (A) A model of hurpin was built using ovalbumin as a scaffold. The conformation of the interhelical C−D loop could not be determined but is shown to indicate its position in the context of the molecule. (B) The hurpin RCL was aligned with RCLs from serpins known to inhibit cysteine proteinases. The sequences have been aligned to emphasize similarities and differences between the main region of the reactive center loop that interacts with the active site of the enzyme. Strict identity between the sequences is indicated by dark gray shading; light gray shading indicates conservation of amino acid type at a given position. The positions of the P_2 and P_1 residues are highlighted by a box, and the P_3' proline residues in hurpin and SCCA-1 are shown in white on black. Note that endopin 2 is cleaved by papain after both T-S and S-S.

Table 1: Inhibitory Profile of Hurpin against Cathepsins

proteinase (final concn)	hurpin (nM)	% inhibition	SI	substrate (final concn)
cathepsin L (10 nM)	50	100	1.7	Cbz-FR-AMC (10 μM)
cathepsin V (10 nM)	80	52	17	Cbz-FR-AMC (10 μM)
cathepsin K (10 nM)	80	0	nd[a]	Cbz-FR-AMC (10 μM)
cathepsin B (10 nM)	200	0	nd	Z-Arg-Arg-AFC (10 μM)
papain (13 nM)	500	6	nd	Cbz-FR-AMC (10 μM)
trypsin (5 nM)	500	<1	>1000	Boc-VPR-AMC (10 μM)
thrombin (10 nM)	500	1	>100	Boc-VPR-AMC (10 μM)
chymotrypsin (10 nM)	500	0	nd	*N*-succinyl-AAPF-AMC (10 μM)
M/N elastase (10 nM)	500	0	nd	*N*-succinyl-APA-AMC (10 μM)
human granzyme B (10 nM)	500	0	nd	Abz-IEPDSSMESK-Dnp (10 μM)

[a] nd = not determined.

less effective compared to the wild-type hurpin. The SI increased to 5.5 and the k_{assoc} decreased approximately 1 order of magnitude to $(4.1 \pm 0.18) \times 10^4$ M^{-1} s^{-1}. The P1 position of cathepsin L is known to be relatively nonselective (*37*); for example, it will accommodate Ala and Phe equally well (*38*). The fact that a relatively minor substitution can have a strong effect on the interaction between hurpin and cathepsin L supports the hypothesis that the interaction between the two is finely balanced.

(B) Hinge Mutant. The flexibility of the hinge regions flanking the RCL of the serpin is essential for the inhibition of serine proteinases. Insertion of the cleaved RCL into β-sheet A and the subsequent stressed to relaxed transition can be prevented in many serpins by substituting the P14 residue (commonly Thr) in the reactive site loop for Arg. Arg at P14 slows the rate of RCL insertion into β-sheet A, abolishes inhibitory activity, and converts the serpin into a substrate. We therefore generated a mutant hurpin protein in which the wild-type P14 residue (^{343}Thr) is changed to Arg. This mutation essentially abolished the catL inhibitory capacity of hurpin. The SI increased to 60 while the k_{assoc} dropped to $(1.3 \pm 0.91) \times 10^3$ M^{-1} s^{-1}. This underscores the importance of the stressed to relaxed transition of the serpin for inhibition of cysteine proteinases.

(C) CD Mutant. The CD interhelical loop is one of the special features of the ov-serpins, and there are several examples in which this region contributes to the biological function of the inhibitor. Our observations that alternatively

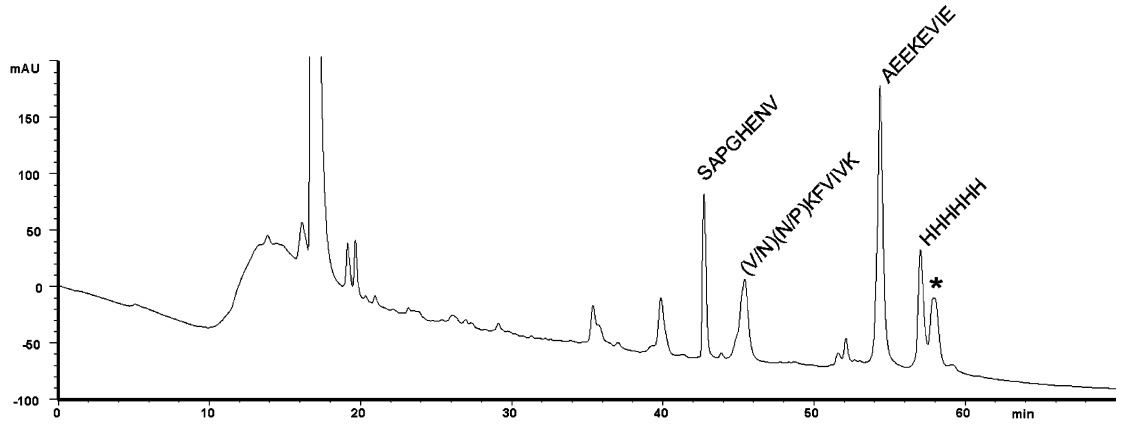

FIGURE 3: Determination of the P1−P1′ bond in hurpin cleaved by catL. Recombinant hurpin was incubated with catL, and cleavage products were separated by HPLC and sequenced. The peak indicated with an asterisk is a known nonpeptidic contaminant.

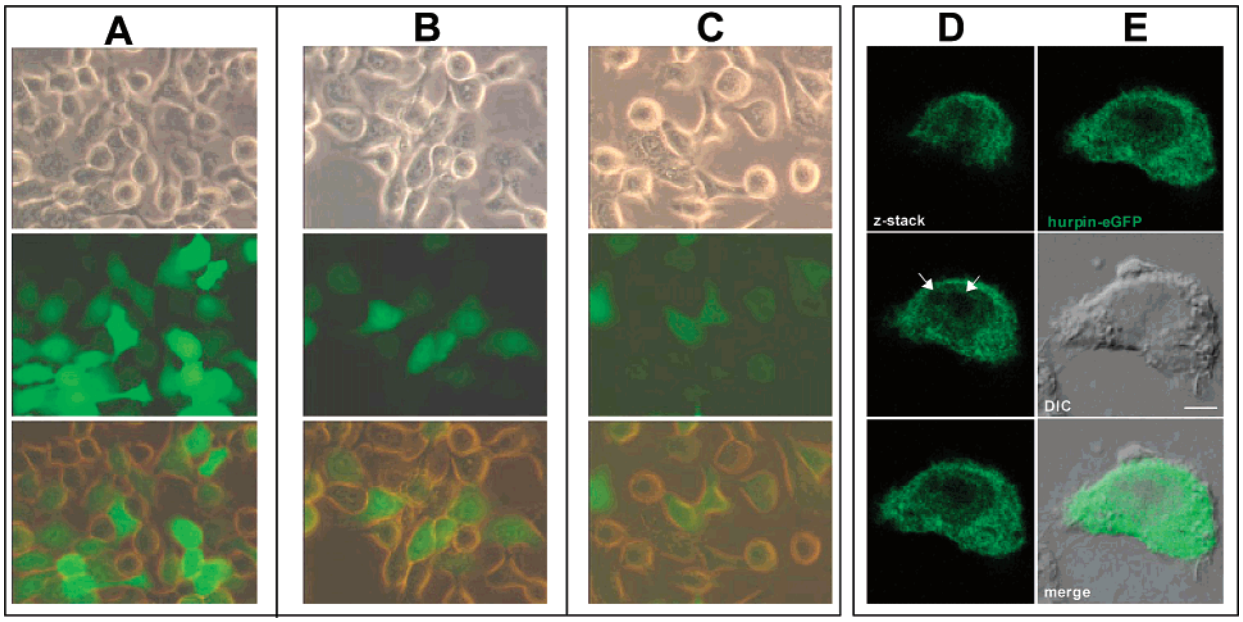

FIGURE 4: Localization of GFP-tagged hurpin in human keratinocytes. Hurpin was transiently expressed as an eGFP fusion protein in HaCaT cells. (A) HaCaT cells after transfection of an eGFP control vector. (B) eGFP fused to the N-terminus of hurpin. (C) eGFP fused to the C-terminus of hurpin. Each row shows (from top to bottom) cells under phase-contrast illumination, epifluorescence images of the same cells, and merged phase-contrast/epifluorescence images. (D) and (E) show CLSM images of HaCaT cells expressing hurpin with a C-terminal eGFP tag. (D) Optical sections of one cell (z-stack). (E) eGFP fluorescence, differential interference contrast (DIC) of the same section, and merged picture (from top to bottom). Arrows indicate positions of nucleoli. The scale bar represents 5 μm.

Table 2: Inhibition of CatL by Wild-Type and Mutant Hurpin

Hurpin form	Sequence	SI	k_{ass} [M^{-1} s^{-1}]
	P17 P14 P1=P1′		
Wild type	^{340}EEGTEAAAATGIGFTVT=SAPGH^{361}	1.7	$4.6 \pm 0.14 \times 10^5$
Thr343Arg	^{340}EEGREAAAATGIGFTVT=SAPGH^{361}	57.0	$1.3 \pm 0.91 \times 10^3$
Thr356Ala	^{340}EEGTEAAAATGIGFTVA=SAPGH^{361}	5.5	$4.1 \pm 0.18 \times 10^4$
ΔCD loop	deletion of the CD interhelical loop	2.0	$2.3 \pm 0.07 \times 10^5$

spliced forms of hurpin with shortened CD loops exist (*8*) and that catL cleaves the CD loop of hurpin (Figure 2) raised the possibility that the CD loop modulates the inhibitory reaction. To test the relevance of the CD interhelical loop of hurpin for inhibiton of catL, we generated a mutant form of hurpin in which this loop is deleted. The SI and k_{assoc} for this CD mutant were 2.1 and $(2.3 \pm 0.07) \times 10^5$ M^{-1} s^{-1} respectively, only slightly different from wild-type hurpin. Obviously the CD interhelical loop does not contribute to hurpin-mediated catL inhibition in vitro. It remains possible that the CD interhelical loop modulates hurpin biological activity in vivo.

Cellular Localization. Recently, many ov-serpins have been shown to be nucleocytoplasmic, even when tagged with green fluorescent protein (GFP) (*39*). To determine the cellular localization of hurpin in keratinocytes, we generated constructs that allow the expression of N- or C-terminal eGFP (enhanced green fluorescent protein) tagged hurpin proteins under the control of a CMV promoter. Since keratinocytes are difficult to transfect using conventional means, we used a novel transfection device (Nucleofector; Amaxa) to obtain the maximum number of HaCaT cells harboring the expression plasmid. With this new technique it was possible to transiently transfect up to 66% of the cells using the pEGFP-C1 control vector (Figure 4A) as determined by FACS analysis (data not shown). As shown in Figure 4B,C, epifluorescence analysis showed predominant cytoplasmic distribution of the hurpin fusion proteins, regardless of the position of the eGFP tag. To confirm the subcellular

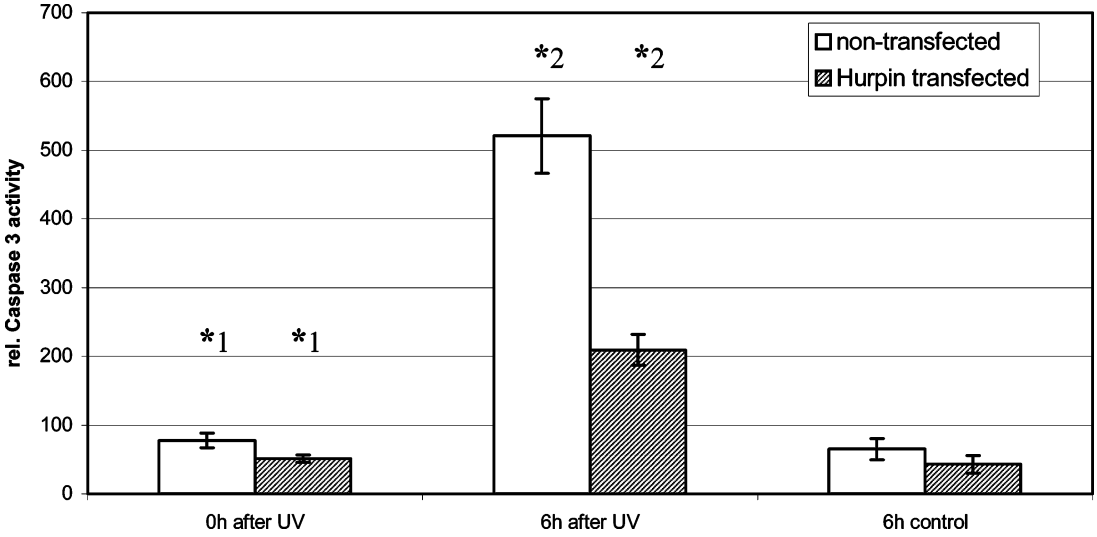

FIGURE 5: Effect of hurpin overexpression on UV-mediated apoptosis. HaCaT cells were transfected with an expression vector comprising the hurpin cDNA under the control of the CMV-promoter. Transfected cells and untransfected control cells were irradiated with 200 J/m^2 UVB. Six hours after irradiation cells were analyzed for caspase 3 activity. Mock-irradiated control cells after 6 h cultivation served as controls (*1, Student's *t*-test, $n = 3$, $\alpha = 0.05$; *2, Student's *t*-test, $n = 3$, $\alpha = 0.001$).

localization of the hurpin−eGFP proteins, transfected HaCaT cells were analyzed by confocal laser scanning microscopy (CLSM). As shown in Figure 4D,E the majority of the eGFP-tagged hurpin is located in the cytoplasm. The fusion protein was also detected in lower amounts in the nucleoplasm and was not present in the nucleoli.

Influence of Hurpin Overexpression on UV-Induced Apoptosis in Keratinocytes. We originally identified hurpin because it is transiently downregulated in UV-irradiated keratinocytes (*4*, *5*). Recent data implicate that UV-irradiation-mediated oxidative stress (*40*) can disrupt lysosomes and cause release of lysosomal hydrolases such as catL (*41*). Furthermore, it has been reported that among other lysosomal proteases catL activates caspase 3, implying that it is a proapoptotic agent (*42*). On the basis of these published findings and our demonstration here that hurpin is an efficient catL inhibitor, we proposed that one of the physiological functions of hurpin is to protect keratinocytes from catL-mediated apoptosis. It follows that overexpression of hurpin may protect cells from UV-mediated stress.

In contrast to the endogenous hurpin gene, hurpin expression driven by a heterologous promoter should not be repressed by UV irradiation. If hurpin is able to block UV-induced apoptosis, overexpression of hurpin in transfected cells should result in resistance to UV-mediated apoptosis. To investigate the effect of hurpin overexpression on apoptosis, we generated stably transfected human keratinocyte (HaCaT) cells carrying a hurpin expression plasmid. The presence of an intact CMV promoter−hurpin coding sequence was confirmed by PCR analysis using genomic DNA from neomycin-resistant cell clones (data not shown).

Semiconfluent cells were then subjected to irradiation with UV light at a sublethal dose of 200 J/m^2 and analyzed 6 h later for caspase 3 activity as an indicator of UV-induced apoptosis. Nontransfected HaCaT cells served as control. While the control cells showed the expected induction of apoptosis 6 h after UV irradiation, the hurpin-transfected cells showed a significantly lower level of apoptosis (Figure 5). These data indicate that hurpin negatively regulates UV-mediated apoptosis in human keratinocytes.

DISCUSSION

Although most serpins inhibit serine proteinases, there is increasing evidence that ov-serpins and viral serpins exhibit "cross-class inhibition" of cysteine proteinases. For example, the virally encoded serpin cytokine response modifier A (crmA) inhibits several caspases, forming complexes which are kinetically reversible and not stable in SDS (*17*). Human SCCA1 and chicken MENT are efficient but relatively nonselective inhibitors of several lysosomal cathespins (*26*, *43*). In this report we have shown that human hurpin is an efficient and selective inhibitor of catL. It is thus the second human serpin shown to be capable of inhibiting papain-like proteinases. Furthermore, the inhibitory profile makes hurpin the most selective serpin inhibitor of cysteine proteinases observed so far. For example, cathepsins L, K, and V demonstrated similar SI values for their interaction with MENT (*26*) and SCCA-1 (*26*, *43*), serpins with P_2 phenylalanine residues, and the P_2 leucine-bearing SQN-5 (*44*). The mouse serpin SQN-5 is a dual mechanistic-class inhibitor of serine and cysteine proteinases (*44*).

In contrast, it appears that hurpin has exploited the differential ability of papain-like cysteine proteinases to hydrolyze substrates with a P_2 valine residue. This difference is highlighted by studies comparing the efficiency with which the substrate Cbz-VVR-AMC is cleaved. Comparison of k_{cat}/K_m values revealed that catL hydrolyzes this substrate 110 times as well as catV (*22*) and 3800 times as well as catK (*45*). Interestingly, this progression mirrors the ability of hurpin to inhibit each of these enzymes: catL is inhibited efficiently, catV poorly, and catK not at all. The fact that valine-containing substrates are suboptimal with respect to phenylalanine-bearing substrates (*22*, *45*) may partly explain the observation that hurpin still has some susbstrate-like character in the reaction with catL. Collectively, these data suggest that hurpin has sacrificed optimal efficiency (SI ~1) for target selectivity.

One other factor that has influenced serpin target specificity is the length of the C-terminal portion of the RCL. For example, a study that made use of antitrypsin mutants found

that catL and catV favored a shorter RCL length than did catK (*25*). Hurpin's RCL is two residues shorter than that of MENT or SCCA-1. However, a wild-type inhibitor more closely related to hurpin, SQN-5, which is also two residues shorter, inhibited cathepsins K, L, and V with roughly equal efficiency (SI ~1). In this light, it seems less likely that C-terminal reactive center loop length plays a significant role in hurpin's selectivity.

Serine proteinase inhibition by serpins involves pronounced conformational change in the inhibitor and distortion of the proteinase. The basis of the serpin conformational change is the flexibility of the hinge region in the RCL (*46*); hence we tested whether this is important for inhibition of catL by hurpin. The results obtained in this study on the hinge mutant of hurpin indicate that the characteristic insertion of the cleaved RCL in β-sheet A is crucial for inhibition of catL by hurpin. This is in accordance with the inhibition of cathepsins by SCCA1 and MENT, where the importance of the mobility of the RCL for the inhibition of cathepsins has been demonstrated (*26*, *35*).

The P1 residue plays a crucial role in determining serpin specificity toward serine proteinases (*10*, *47*). By alignment with other serpins the putative P1−P1′ bond within the hurpin RCL was predicted as ^{356}Thr−^{357}Ser. Identification of the cleavage site for catL by peptide sequencing confirmed that the inhibitor is hydrolyzed by catL between these residues and suggests that reaction follows the standard inhibitory mechanism. Consistent with this observation, alteration of the P1 residue from Thr to Ala significantly reduced but did not completely abrogate the inhibitory activity of hurpin toward catL. This indicates that while the P1 residue is important for the catL inhibition, it is not a critical determinant of this proteinase−inhibitor interaction.

Like many serine proteinase−serpin interactions, residues surrounding the P1 residue are likely to play a role in binding affinity (*21*). Thus it is assumed that, for inhibition of cathepsins, the P2 residue of the RCL might play an important role and, indeed, those serpins which have been shown to inhibit cathepsins to date, such as MENT and SCCA1, usually have a hydrophobic amino acid in the P2 position (*26*, *35*). Thus it is likely that the P2 Val residue in the RCL of hurpin is important in promoting the interaction with catL. The contribution of residues outside the P1−P1′ bond has been illustrated in attempts to convert the serine proteinase inhibitor SCCA2 into a cathepsin inhibitor like SCCA1. No single mutation was able to change the specificity of SCCA2, but rather a combination of mutations in the P1, P3′, P4′, and P11′ positions was required (*34*).

The interhelical loop between helix C and helix D is another characteristic feature of ov-serpins (*7*, *10*), and it has been shown that this region can influence biological activity independently of the interaction of the RCL with a cognate proteinase (*11*). For example, both MENT and bomapin contain a nuclear targeting domain in this region (*12*, *48*), and it is the site of transglutamination in PAI-2 (*49*). We have described two hurpin variants that show alterations in exon 3, which forms the interhelical loop (*8*). In both cases, we identified the use of a different 5′ splice site between exon 3 and intron C as the source of the observed variations. Given our observation that cleavage of the CD loop occurs during the catL−hurpin interaction, it was especially interesting to determine if the hurpin CD loop is involved in the inhibition of catL. However, deletion of the complete CD loop did not alter the inhibitory capacity of the serpin toward catL. This does not preclude a role for the CD loop in hurpin biology, but at least for the in vitro cross-class inhibition of catL it does not seem to be important.

Our data strongly suggest that lysosomal catL is a physiologically relevant target for hurpin. Recent evidence has begun to show that lysosomal enzymes have a role beyond bulk protein degradation in the lysosomal compartment (*50*). The release of cathepsins from lysosomes and the induction of apoptosis have been reported to follow cellular stress (*41*, *51*, *52*). CatL together with other lysosomal enzymes is involved in the activation of caspase 3 (*42*), and induction of cell death may involve the proapoptotic mediator Bid (*53*).

The induction of apoptosis in epidermal keratinocytes by UVB irradiation is well established (*54*, *55*) and involves oxidative stress that destabilizes lysosomes (*40*, *56*, *57*). Hurpin was initially identified due to its transient transcriptional downregulation following UV irradiation of human keratinocytes (*4*). Building on the new results presented in this report, we propose that a biological role of hurpin is to control catL released from lysosomes and prevent apoptosis in human keratinocytes. We envisage that during UV irradiation lysosomal enzymes are released into the cytoplasm of the keratinocytes. Cytoplasmic hurpin is depleted by interaction with lysosomal catL, and new synthesis of hurpin is prevented by transcriptional shutdown and rapid degradation of hurpin mRNA. The resulting excess of uninhibited catL generates caspase 3 directly, or indirectly via Bid, and thus contributes to apoptosis.

Several lines of evidence support this model. First, the majority of hurpin is localized in the cytoplasm of keratinocytes and is thus poised to interact with proteolytic enzymes escaping from leaky lysosomes. Second, HaCaT cells overexpressing hurpin show reduced apoptosis in response to UV irradiation. Finally, a recent report on catL-deficient mice shows that lack of catL leads to periodic hair loss, epidermal hyperplasia, ancanthosis, and hyperkeratosis (*58*). These pathologic alterations are characteristic of psoriatic skin lesions (*59*). Hurpin and SCCA1 are overexpressed in psoriasis (*5*, *60*), and both are inhibitors of catL (this report; *43*). Overexpression of these serpins could therefore cause phenotypic catL deficiency in psoriasis and may underpin the antiapoptotic, hyperproliferative phenotype of psoriatic keratinocytes.

ACKNOWLEDGMENT

We thank Dr. D. Brömme for generously providing purified cathepsins and recombinant cathepsin expression systems. We also thank M. Walz, B. Lysa, U. Tartler, and P. Genutt for supporting the transfection of HaCaT cells for CLSM.

REFERENCES

1. Schulze, A. J., Huber, R., Bode, W., and Engh, R. A. (1994) *FEBS Lett. 344*, 117−124.
2. Wright, H. T., and Scarsdale, J. N. (1995) *Proteins 22*, 210−225.

3. Huntington, J. A., Read, R. J., and Carrell, R. W. (2000) *Nature 407*, 923−926.
4. Abts, H. F., Breuhahn, K., Michel, G., Köhrer, K., Esser, P., and Ruzicka, T. (1997) *Photochem. Photobiol. 66*, 363−367.
5. Abts, H. F., Welss, T., Mirmohammadsadegh, A., Köhrer, K., Michel, G., and Ruzicka, T. (1999) *J. Mol. Biol. 293*, 29−39.
6. Spring, P., Nakashima, T., Frederick, M., Henderson, Y., and Clayman, G. (1999) *Biochem. Biophys. Res. Commun. 264*, 299−304.
7. Remold-O'Donnell, E. (1993) *FEBS Lett. 315*, 105−108.
8. Abts, H. F., Welss, T., Scheuring, S., Scott, F. L., Irving, J. A., Michel, G., Bird, P. I., and Ruzicka, T. (2001) *DNA Cell Biol. 20*, 123−131.
9. Nakashima, T., Pak, S. C., Silverman, G. A., Spring, P. M., Frederick, M. J., and Clayman, G. L. (2000) *Biochim. Biophys. Acta 1492*, 441−446.
10. Huber, R., and Carrell, R. W. (1989) *Biochemistry 28*, 8951−8966.
11. Jensen, P. H., Jensen, T. G., Laug, W. E., Hager, H., Gliemann, J., and Pepinsky, B. (1996) *J. Biol. Chem. 271*, 26892−26899.
12. Chuang, T. L., and Schleef, R. R. (1999) *J. Biol. Chem. 274*, 11194−11198.
13. Schick, C., Kamachi, Y., Bartuski, A. J., Cataltepe, S., Schechter, N. M., Pemberton, P. A., and Silverman, G. A. (1997) *J. Biol. Chem. 272*, 1849−1855.
14. Hopkins, P. C., and Whisstock, J. (1994) *Science 265*, 1893−1894.
15. Potempa, J., Korzus, E., and Travis, J. (1994) *J. Biol. Chem. 269*, 15957−15960.
16. Simonovic, M., Gettins, P. G. W., and Volz, K. (2000) *Protein Sci. 9*, 1423−1427.
17. Zhou, Q., Snipas, S., Orth, K., Muzio, M., Dixit, V. M., and Salvesen, G. S. (1997) *J. Biol. Chem. 272*, 7797−7800.
18. Deng, W. P., and Nickoloff, J. A. (1992) *Anal. Biochem. 200*, 81−88.
19. Sun, J., Coughlin, P., Salem, H. H., and Bird, P. (1995) *Biochim. Biophys. Acta 1252*, 28−34.
20. Mast, A. E., Enghild, J. J., Nagase, H., Suzuki, K., Pizzo, S. V., and Salvesen, G. (1991) *J. Biol. Chem. 266*, 15810−15816.
21. Sun, J., Whisstock, J. C., Harriott, P., Walker, B., Novak, A., Thompson, P. E., Smith, A. I., and Bird, P. I. (2001) *J. Biol. Chem. 276*, 15177−15184.
22. Brömme, D., Li, Z., Barnes, M., and Mehler, E. (1999) *Biochemistry 38*, 2377−2385.
23. Linnevers, C. J., McGrath, M. E., Armstrong, R., Mistry, F. R., Barnes, M. G., Klaus, J. L., Palmer, J. T., Katz, B. A., and Brömme, D. (1997) *Protein Sci. 6*, 919−921.
24. Barrett, A. J., Kembhavi, A. A., Brown, M. A., Kirschke, H., Knight, C. G., Tamai, M., and Hanada, K. (1982) *Biochem. J. 201*, 189−198.
25. Irving, J. A., Pike, R. N., Dai, W., Brömme, D., Worrall, D. M., Silverman, G. A., Coetzer, T. H., Dennison, C., Bottomley, S. P., and Whisstock, J. C. (2002) *Biochemistry 41*, 4998−5004.
26. Irving, J. A., Shushanov, S. S., Pike, R. N., Popova, E. Y., Brömme, D., Coetzer, T. H., Bottomley, S. P., Boulynko, I. A., Grigoryev, S. A., and Whisstock, J. C. (2002) *J. Biol. Chem. 277*, 13192−13201.
27. Morrison, J. F., and Walsh, C. T. (1988) *Adv. Enzymol. Relat. Areas Mol. Biol. 61*, 201−301.
28. Rovelli, G., Stone, S. R., Guidolin, A., Sommer, J., and Monard, D. (1992) *Biochemistry 31*, 3542−3549.
29. Boukamp, P., Petrussevska, R. T., Breitkreutz, D., Hornung, J., Markham, A., and Fusenig, N. E. (1988) *J. Cell Biol. 106*, 761−771.
30. Abts, H. F., Welss, T., Breuhahn, K., and Ruzicka, T. (2000) in *Stress Response. Methods and Protocols* (Keyse, S. M., Ed.) pp 347−366, Humana Press, Totowa, NJ.
31. Stein, P. E., Leslie, A. G., Finch, J. T., and Carrell, R. W. (1991) *J. Mol. Biol. 221*, 941−959.
32. Sali, A., and Blundell, T. L. (1993) *J. Mol. Biol. 234*, 779−815.
33. Hopkins, P. C., Carrell, R. W., and Stone, S. R. (1993) *Biochemistry 32*, 7650−7657.
34. Luke, C., Schick, C., Tsu, C., Whisstock, J. C., Irving, J. A., Brömme, D., Juliano, L., Shi, G. P., Chapman, H. A., and Silverman, G. A. (2000) *Biochemistry 39*, 7081−7091.
35. Schick, C., Brömme, D., Bartuski, A. J., Uemura, Y., Schechter, N. M., and Silverman, G. A. (1998) *Proc. Natl. Acad. Sci. U.S.A. 95*, 13465−13470.
36. Travis, J., and Salvesen, G. S. (1983) *Annu. Rev. Biochem. 52*, 655−709.
37. Brocklehurst, K., Willenbrock, F., and Salih, E. (2002) in *Cysteine proteinases* (Neuberger, A., and Brocklehurst, K., Eds.) Elsevier, Amsterdam.
38. Kirschke, H., and Shaw, E. (1981) *Biochem. Biophys. Res. Commun. 101*, 454−458.
39. Bird, C. H., Blink, E. J., Hirst, C. E., Buzza, M. S., Steele, P. M., Sun, J., Jans, D. A., and Bird, P. I. (2001) *Mol. Cell. Biol. 21*, 5396−5407.
40. Peus, D., Vasa, R. A., Meves, A., Pott, M., Beyerle, A., Squillace, K., and Pittelkow, M. R. (1998) *J. Invest. Dermatol. 110*, 966−971.
41. Brunk, U. T., Neuzil, J., and Eaton, J. W. (2001) *Redox Rep. 6*, 91−97.
42. Ishisaka, R., Utsumi, T., Yabuki, M., Kanno, T., Furuno, T., Inoue, M., and Utsumi, K. (1998) *FEBS Lett. 435*, 233−236.
43. Schick, C., Pemberton, P. A., Shi, G. P., Kamachi, Y., Cataltepe, S., Bartuski, A. J., Gornstein, E. R., Brömme, D., Chapman, H. A., and Silverman, G. A. (1998) *Biochemistry 37*, 5258−5266.
44. Al Khunaizi, M., Luke, C. J., Askew, Y. S., Pak, S. C., Askew, D. J., Cataltepe, S., Miller, D., Mills, D. R., Tsu, C., Brömme, D., Irving, J. A., Whisstock, J. C., and Silverman, G. A. (2002) *Biochemistry 41*, 3189−3199.
45. Brömme, D., Okamoto, K., Wang, B. B., and Biroc, S. (1996) *J. Biol. Chem. 271*, 2126−2132.
46. Whisstock, J., Skinner, R., and Lesk, A. M. (1998) *Trends Biochem. Sci. 23*, 63−67.
47. Bode, W., and Huber, R. (1992) *Eur. J. Biochem. 204*, 433−451.
48. Grigoryev, S. A., Bednar, J., and Woodcock, C. L. (1999) *J. Biol. Chem. 274*, 5626−5636.
49. Jensen, P. H., Schuler, E., Woodrow, G., Richardson, M., Goss, N., Hojrup, P., Petersen, T. E., and Rasmussen, L. K. (1994) *J. Biol. Chem. 269*, 15394−15398.
50. Chapman, H. A., Riese, R. J., and Shi, G. P. (1997) *Annu. Rev. Physiol 59*, 63−88.
51. Brunk, U. T., and Svensson, I. (1999) *Redox Rep. 4*, 3−11.
52. Antunes, F., Cadenas, E., and Brunk, U. T. (2001) *Biochem. J. 356*, 549−555.
53. Stoka, V., Turk, B., Schendel, S. L., Kim, T. H., Cirman, T., Snipas, S. J., Ellerby, L. M., Bredesen, D., Freeze, H., Abrahamson, M., Brömme, D., Krajewski, S., Reed, J. C., Yin, X. M., Turk, V., and Salvesen, G. S. (2001) *J. Biol. Chem. 276*, 3149−3157.
54. Leverkus, M., Yaar, M., and Gilchrest, B. A. (1997) *Exp. Cell Res. 232*, 255−262.
55. Schwarz, A., Bhardwaj, R., Aragane, Y., Mahnke, K., Riemann, H., Metze, D., Luger, T. A., and Schwarz, T. (1995) *J. Invest. Dermatol. 104*, 922−927.
56. Scharffetter-Kochanek, K., Wlaschek, M., Brenneisen, P., Schauen, M., Blaudschun, R., and Wenk, J. (1997) *Biol. Chem. 378*, 1247−1257.
57. Zhang, Q. S., Maddock, D. A., Chen, J. P., Heo, S., Chiu, C., Lai, D., Souza, K., Mehta, S., and Wan, Y. S. (2001) *Int. J. Oncol. 19*, 1057−1061.
58. Roth, W., Deussing, J., Botchkarev, V. A., Pauly-Evers, M., Saftig, P., Hafner, A., Schmidt, P., Schmahl, W., Scherer, J., Anton-Lamprecht, I., Von Figura, K., Paus, R., and Peters, C. (2000) *FASEB J. 14*, 2075−2086.
59. Camp, R. (1992) in *Textbook of Dermatology* (Champion, R., Burton, J., and Ebling, F., Eds.) pp 1391−1457, Blackwell, Oxford.
60. Rivas, M. V., Jarvis, E. D., Morisaki, S., Carbonaro, H., Gottlieb, A. B., and Krueger, J. G. (1997) *J. Invest. Dermatol. 108*, 188−194.

BI027307Q